MesoFT: Mesoscopic Structure and Orientation with Fiber Tracking

Marco Reisert[1], Matthias Weigel[1], Els Fieremans[2], Valerij G. Kiselev[1], and Dmitry S Novikov[2]
[1]*Dpt. of Radiology, Medical Physics, University Medical Center Freiburg, Freiburg, BW, Germany,* [2]*Center for Biomedical Imaging, Dpt. of Radiology, New York University School of Medicine, New York, NY, United States*

Target Audience: *Biophysical Mechanisms of Diffusion-Weighted Signal* community and *Fiber Tractography* community

Purpose: To present the MesoFT framework that unifies sub-voxel modeling of dMRI signal at the mesoscopic scale with multi-voxel connectivity achieved with global fiber tracking

Methods: The greatest challenge of quantifying tissue structure with MRI is to bridge the three-orders-of-magnitude gap between a *macroscopic* measurement (mm resolution) and the *mesoscopic* tissue architecture at the µm level. Given the limitations of a clinical dMRI scan, the inverse problem of quantifying tissue structure in every voxel is highly ill-posed. To regularize it, we propose to utilize information about the source of the underlying anisotropy: the fibrous structure of the neurites, i.e. axons in white matter and both axons and dendrites in gray matter. As the neurites stretch beyond voxel dimensions, it is natural to reconstruct their directions *simultaneously* with quantifying tissue structure in each voxel in a self-consistent way.

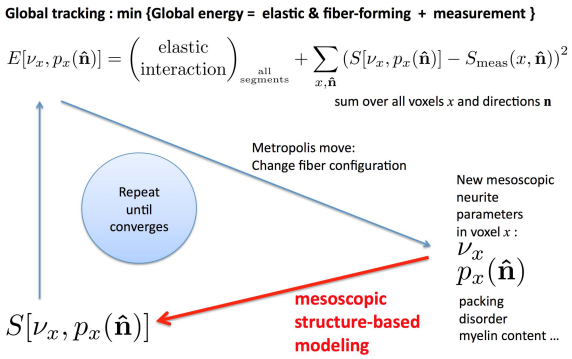

Fig. 1: Schematic of the MesoFT: Global tracking, based on energy minimization (likelihood maximization) of the fiber-forming segments in the presence of dMRI-measured signal, is combined with modelling of dMRI signal from each segment representing mesoscopic axonal structure of the neurites. The convergence is achieved iteratively.

The *global nature* of the fiber tracking algorithm [1] used here is crucial for incorporating realistic mesoscopic modeling. Indeed, the wide variety of alternative approaches [2] to tractography have been local, based for the most part on following the direction of the principal eigenvalue of the diffusion tensor, either deterministically or probabilistically. Such approaches are prone to error accumulation along the reconstructed paths. Global tracking, on the other hand, is based on global energy minimization over the whole brain (Fig. 1) for a system of interacting segments that prefer polymerization to form fibers under simulated annealing. This procedure naturally averages over uncorrelated noise in different voxels and therefore is much more robust [2]. But more importantly, global tractography by design needs to model the signal $S[\nu_x,\ p_x(\mathbf{n})]$ from the collection of segments in each voxel at each Metropolis-Hastings step of the segments' rearrangement, in order to compare it with the measured signal S_{meas}, Fig. 1. To achieve realistic mesoscopic modeling, as the first step, here we incorporate the accepted model of narrow cylinders for the neurites [3,4], in which each neurite contributes to the signal with the diffusion coefficient D_a and zero diffusivity in the transverse directions. The extra-axonal signal with a variable water fraction is characterized by a generic diffusion tensor $\boldsymbol{D}^e$. While the positions of neurite segments were optimized in continuous space, the extra-axonal tensor was defined per voxel.

Experiment: The brain in a 30 y/o male healthy volunteer was measured with a standard HARDY sequence, employing four *b*-factor shells from b=0.5 (29 directions) to b=2 ms/µm^2 (115 directions) filling q-space nearly uniformly. Here we present our results for white matter (WM) and corpus callosum (CC).

Results: Figure 2 shows the obtained distribution of eigenvalues of extra-axonal tensor $\boldsymbol{D}^e$ in WM and Fig. 3 in a region in the CC with unidirectional fibers. Figure 4 shows the distribution of the tortuosity of extra-axonal tensor defined as $2\lambda_1/(\lambda_\square+\lambda_\square)$ both across whole WM and in CC (white matter counts are scaled by 10^{-3}).

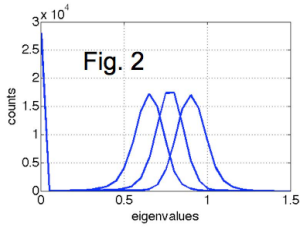

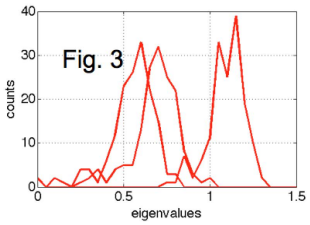

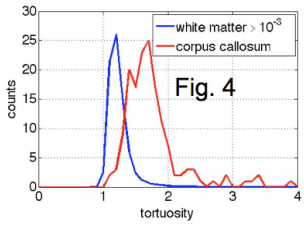

Discussion: The distribution of eigenvalues of extra-axonal diffusion tensor (Figs. 2, 3) shows a notable anisotropy, suggesting that approximating $\boldsymbol{D}^e$ with an isotropic tensor is generally not sufficient. As expected, this anisotropy is more pronounced in CC with one large and two small eigenvalues (diffusion practically isotropic transverse to CC). However, the eigenvalues and the extra-axonal tortuosity due to the presence of axons appear to be somewhat smaller than reported previously using the DKI-based modeling [5]. The tortuosity is another hallmark of the dominance of densely packed WM fibers in CC relative to most other WM regions.

The present combined approach can be viewed as a regularization of sub-voxel modeling via global multi-voxel connectivity. In contrast to using FT as a guide for comparing other MR metrics [6], MesoFT employs the feedback from the dMRI signal onto delineation of tracts. From the point of view of fiber tracking, it enables more adequate account for the extra-axonal signal than via the commonly used subtraction of the isotropic signal component [1]. In general, due to the iterative nature of the procedure, when MesoFT converges, we obtain the physically motivated fiber directions, connections, voxel-wise neurite densities, and, in principle, can incorporate other mesoscopic parameters such as the degree of myelination [7,8]. By design, this framework can be further improved by advancing the mesoscopic modeling, and adding more features (packing types [9], effects of paramagnetic ions on the apparent diffusion metrics [10], likelihood function for nongaussian MR noise etc.) as additional modules in Fig. 1.

References: [1] M Reisert *et al.*, *NeuroImage* 54, 955 (2011). [2] P Fillard *et al.*, *NeuroImage* 56, 220 (2011). [3] Y Assaf *et al.*, *MRM* 52, 965 (2004). [4] SN Jespersen *et al.*, *NeuroImage* 34, 1473 (2007); *NeuroImage* 49, 205 (2010). [5] E Fieremans et al., *NeuroImage* 58, 177 (2011). [6] S Bells *et al.*, *Proc ISMRM* 19, 678 (2011). [7] DS Novikov and E Fieremans, *Proc ISMRM* 20, 1829 (2012). [8] E Fieremans *et al.*, *Proc ISMRM* 20, 465 (2012). [9] DS Novikov *et al.*, http://arxiv.org/abs/1210.3014. [10] DS Novikov *et al.*, *Proc ISMRM* 20, 2071 (2012).